Key Engineering Materials
ISSN: 1662-9795, Vol. 926, pp 316-322
doi:10.4028/p-1r2x8g

Submitted: 2021-12-08
Accepted: 2022-02-18
Online: 2022-07-22

Assessing the Accuracy of Different Remapping Methods in Adaptive Mesh Refinement

B.M. Marques[1,a*], D.M. Neto[1,b] and J.L. Alves[2,c]

[1]CEMMPRE, Department of Mechanical Engineering, University of Coimbra, Pinhal de Marrocos, 3030-788 Coimbra, Portugal

[2]Microelectromechanical Systems Research Unit, University of Minho, Campus de Azurém, Guimarães, 4800-058, Portugal

[a]bruno.marques@uc.pt, [b]diogo.neto@dem.uc.pt, [c]jlalves@dem.uminho.pt

Keywords: Finite element method; Remapping state variables; Shape functions; Dual Kriging.

Abstract. Additive manufacturing of metals has attracted much attention over the last years, promoting the development of several computational models for numerical simulation of the laser powder bed fusion (LPBF) process. Nevertheless, the finite element analysis of the LPBF process requires a large computational time. Thus, adaptive mesh refinement strategies are commonly adopted to reduce computational cost, which require some remapping procedure to transfer the state variables from the old mesh to the new one. The present study analyses two different remapping algorithms, namely the Inverse Isoparametric Mapping (IIM) and the Dual Kriging (DK) method. The IIM method uses the shape functions of the finite elements, while the DK method provides an explicit parametric interpolation. The case study adopted covers both coarsening and refinement procedures, using a mathematical function to define the mapped state variable. The accuracy of the remapping methods was lower in the refinement in comparison with the coarsening procedure. The error in the approximation is lower using the DK method in comparison with the IIM method. However, the IIM method does not suffer from error propagation in successive stages of either refinement/derefinement or coarsening/decoarsening.

Introduction

Additive manufacturing of metals has attracted much attention over the last few years [1], promoting the development of several computational models for numerical simulation of the laser powder bed fusion (LPBF) process. Nevertheless, the finite element analysis of the LPBF process requires a large computational time due to the multiphysics phenomena across multiple scales [2]. Furthermore, the accuracy of the numerical solution and the computational time strongly depends on the finite element mesh adopted in the numerical analysis [3]. Thus, remeshing procedures are commonly adopted to reduce the computational cost by refining only the regions where a fine mesh is required [4]. These strategies are employed in intermediate phases during computation, where the distribution and/or quantity of nodes/elements of the finite element mesh is modified. Remeshing can be further classified into refinement or coarsening procedures, depending on whether the number of nodes/elements is increased or decreased, respectively, locally or across the entire mesh domain.

Variable Remapping

During remeshing, nodes/elements are removed, added or have their spatial position changed. Therefore, a variable remapping procedure must be performed to transfer the nodal and state variables from the original mesh to the required locations in order to preserve the evolution of the historical-dependent variables [5]. Several types of variable remapping methods are available in the literature. Jiao and Heath [6] define five categories: pointwise interpolation and extrapolation, area-weighted averaging, mortar elements methods, and specialised methods. This study is focused only on pointwise interpolation and extrapolation, namely the inverse isoparametric mapping (IIM) and the Dual Kriging (DK) method.

When mapping nodal-based data (e.g. displacements), a simple and consistent approach is to use the element shape functions. However, the transfer of integration point-based variables (state variables) often requires extrapolation techniques associated with the introduction of artificial numerical errors. Additionally, since the true distribution of the field variables is unknown, the risk of the violation of constitutive relations on the new mesh is present and, in such cases, may require additional equilibrium iterations [5].

Inverse isoparametric mapping. Inverse isoparametric mapping is a widespread method for interpolating using the inverted element shape functions [7,8]. For an isoparametric hexahedral element, the shape functions are given by

$$\tilde{N}_i = \sum_{i=1}^{8} \frac{1}{8}\left(1+\xi_i\xi\right)\left(1+\eta_i\eta\right)\left(1+\zeta_i\zeta\right), \tag{1}$$

where $\tilde{N}_i$ is the shape function associated with the node *i* and (ξ,η,ζ) denotes the element's canonical coordinate system.

When remapping state variables, this approach contains 3 stages, while the third step is skipped in the case of remapping nodal variables. In the first stage, the state variables present in the Gauss points of the donor mesh are extrapolated to the nodes of the donor mesh. Considering a scalar state variable *α*, the transfer operation for a generic node *i* is given by

$$\alpha_i^D = \sum_{ig=1}^{n_{ng^D}} \left[\tilde{N}_i^{e^D}\left(\xi^{ig},\eta^{ig},\zeta^{ig}\right)\right]^{-1} \alpha_{ig}^D, \tag{2}$$

where α_{ig}^D is the state variable at the *ig* Gauss point of the donor mesh (*D*), n_{ng^D} is the number of Gauss points of the finite element e^D of the donor mesh, and $\tilde{N}_i^{e^D}$ is the shape function associated with the node i, calculated on the *ig* Gauss point of the e^D finite element. Since a single node can be shared by several finite elements, the process is repeated for each element and the final nodal value is obtained by arithmetic average.

In the second stage, the state variables are transferred from the donor mesh nodes to the target mesh nodes by interpolation, using the donor element's shape functions. This transfer operation is defined by

$$\alpha_j^T = \sum_{i=1}^{n_{ne^D}} \tilde{N}_i^{e^D}\left(\xi^j,\eta^j,\zeta^j\right)\alpha_i^D, \tag{3}$$

where α_j^T is the state variable calculated at the *j* node of the target mesh (T), n_{ne^D} is the number of nodes of the finite element e^D, and $\tilde{N}_i^{e^D}$ is the shape function associated with the node *i* of the donor finite element e^D, calculated at the *j* node of the target mesh.

The third stage comprises the variable transfer from the nodes to the Gauss points of the target mesh, applying the shape functions of the target finite elements, given by

$$\alpha_{ig}^T = \sum_{i=1}^{n_{ne^T}} \tilde{N}_j^{e^T}\left(\xi^{ig},\eta^{ig},\zeta^{ig}\right)\alpha_i^T, \tag{4}$$

where α_{ig}^T is the state variable calculated at the *ig* Gauss point of the target mesh, n_{ne^T} is the number of nodes of the finite element e^T, and $\tilde{N}_j^{e^T}$ is the shape function associated with the node *J*, calculated on the *ig* Gauss point of the e^T finite element.

Dual Kriging. Dual Kriging (DK) is an unbiased linear estimator, capable of giving back the known values at the seed points [9]. The DK interpolator has the following form

$$F\left(X_o,Y_o,Z_o\right) = C_0 + C_1X_o + C_2Y_o + C_3Z_o + \sum_{J=1}^{N}\lambda_J K\left(h_{0J}\right), \tag{5}$$

where $F\left(X_o,Y_o,Z_o\right)$ is the interpolated value associated with the point $\left(X_o,Y_o,Z_o\right)$ in space, *N* is the number of seed points, C_0, C_1, C_2, C_3 and λ_J are interpolation parameters and $K\left(h_{0J}\right)$ is the covariance function value associated with the Euclidean norm between point *0* and point *J*.

The covariance function can assume different forms [9]. However, only two forms were explored in the present study, a linear spline

$$K(H)=1-(H/L), \tag{6}$$

and a cubic spline

$$K(H)=1-3(H/L)^2+2(H/L)^3, \tag{7}$$

where H is the Euclidean norm between point M and point J ($H=\sqrt{h_{MJ}^2}$) and L is the maximum value of H.

In order to obtain the values of C_0, C_1, C_2, C_3 and λ_J, the following system of linear equations must be solved

$$\begin{bmatrix} & & & & & 1 & X_1 & Y_1 & Z_1 \\ & & & & & 1 & X_2 & Y_2 & Z_2 \\ & & [K_{MJ}] & & & 1 & X_3 & Y_3 & Z_3 \\ & & & & & \vdots & \vdots & \vdots & \vdots \\ & & & & & 1 & X_N & Y_N & Z_N \\ 1 & 1 & 1 & \cdots & 1 & & & & \\ X_1 & X_2 & X_3 & \cdots & X_N & & 0_{4,4} & & \\ Y_1 & Y_2 & Y_3 & \cdots & Y_N & & & & \\ Z_1 & Z_2 & Z_3 & \cdots & Z_N & & & & \end{bmatrix} \begin{Bmatrix} \lambda_1 \\ \lambda_2 \\ \lambda_3 \\ \vdots \\ \lambda_N \\ C_0 \\ C_1 \\ C_2 \\ C_3 \end{Bmatrix} = \begin{Bmatrix} F(X_1,Y_1,Z_1) \\ F(X_2,Y_2,Z_2) \\ F(X_3,Y_3,Z_3) \\ \vdots \\ F(X_N,Y_N,Z_N) \\ 0 \\ 0 \\ 0 \\ 0 \end{Bmatrix} \tag{8}$$

where $[K_{MJ}]$ is a square submatrix fully populated containing the values of the covariance between all pairs of seed points and $0_{4,4}$ is a 4 by 4 null matrix.

Numerical Example

The accuracy of the presented remapping methods is assessed using a simple example. The discretisation domain is a cube of edge size equal to 2, centred at the origin of the Cartesian referential and edges parallel to the axis. The values of the state variable are defined according to the trigonometric function

$$f(x,y,z)=\cos(\pi x)\times\cos(\pi y)\times\cos(\pi z), \tag{9}$$

where x, y and z range between -1 and 1. Thus, state variable given by Eq. (1) is always in the range [-1, 1]. A 3D representation of the function over the mesh domain is present in Fig. 1 (a), which highlights the strong gradient of the function value in all directions.

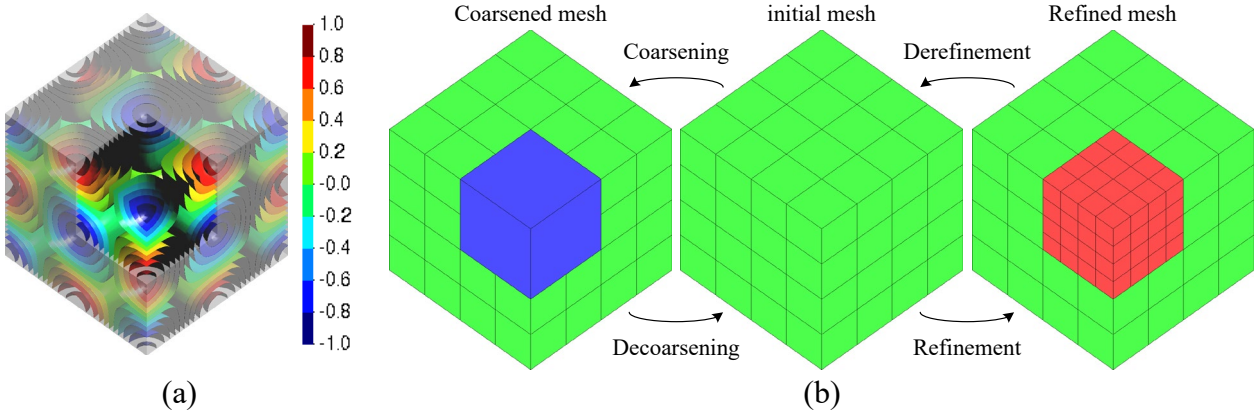

Fig. 1 – Definition of the numerical example: (a) distribution of the state variable; (b) finite element meshes used in the remapping procedure.

Fig. 1 (b) presents the initial mesh composed of 64 hexahedral elements arranged in a 4×4×4 setup. A coarsening procedure has been applied on an eighth of the geometry, converting 8 finite elements into a single one (blue), as shown in Fig. 1 (b). On the other hand, a refinement procedure has been

applied on the same region, converting 8 finite elements into 64 finite elements (red), as shown in Fig. 1 (b). The procedure carried out to return from the coarsened mesh to the initial mesh is called decoarsening while the return to the initial mesh from the refined mesh is called derefinement.

Results and Discussion

In order to assess the accuracy of the previously described remapping methods, the absolute error is evaluated in each Gauss point. The error is defined as the difference between the approximated and the analytical value of the of the state variable given by Eq. (1). Both coarsening and refinement procedures are analysed.

Coarsening procedure. The error in each Gauss point of the coarsened mesh (blue element in Fig. 1 (b)) is presented in Fig. 2 (a), comparing the IIM and the DK methods. The error obtained from the application of the DK method with a cubic spline covariance function is negligible. However, when a linear spline covariance function is adopted, the error increases significatively to about 0.02. On the other hand, the IIM method provides the worse solution, presenting an error about ten times larger than in the DK with a linear spline covariance function.

Fig. 2 (b) presents the error distribution obtained with the IIM method. The error is evaluated only at the Gauss points and then extrapolated to the nodes using the element's shape functions. Therefore, the error is significantly increased from the Gauss points to the nodes. The minimum remapping error (negative) occur in places where the state variable is positive (maximum), while the maximum error (positive) occurs in zones where the state variable is negative (minimum). The distribution obtained with the DK method is identical.

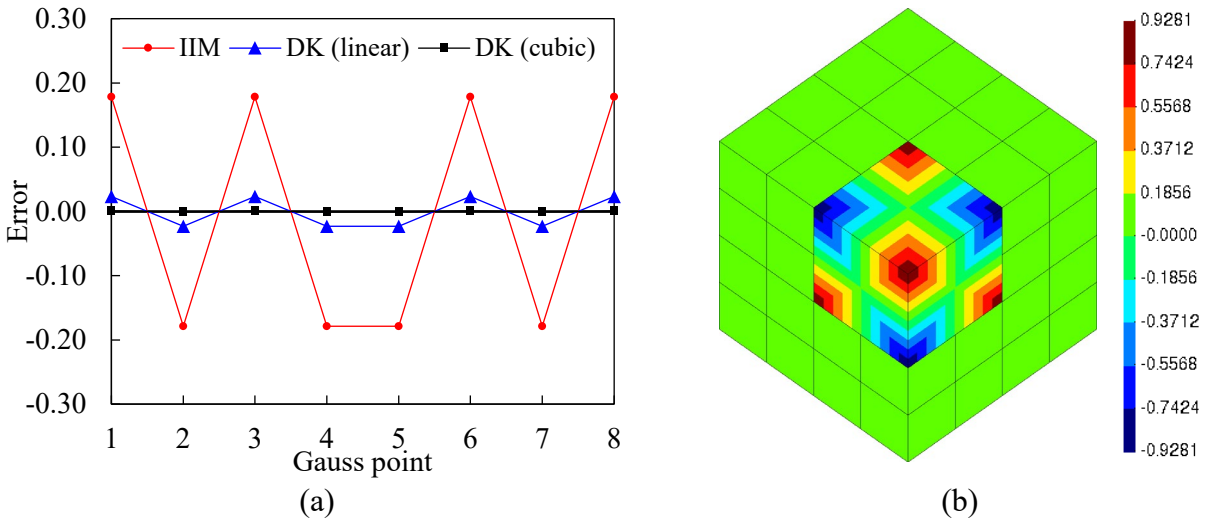

Fig. 2 – Coarsening procedure: (a) error evaluated in the Gauss points; (b) error distribution obtained with the IIM method.

Refinement procedure. Fig. 3 presents the average error of each element subjected to refinement (highlighted in red in Fig. 1 (b)). The DK method with linear spline covariance function provides the worse estimative, i.e. the highest and lowest error values. The error obtained using the IIM method is identical to the one obtained with the DK with cubic spline covariance function. Adopting the IIM method, most of the Gauss points (87.5%) have error values close to zero (<0.003). However, the average absolute error values were more significant.

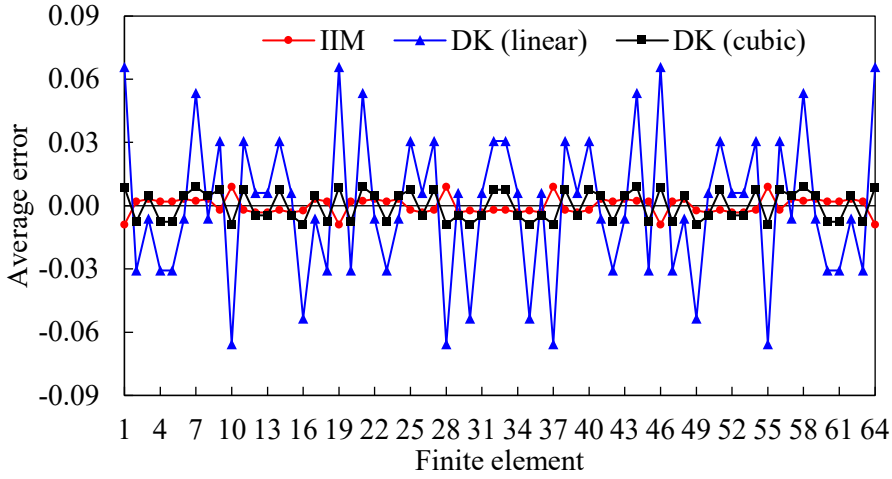

Fig. 3 – Average error in each element after the refinement procedure.

Fig. 4 presents both the maximum and the minimum error values observed in each finite element after the refinement procedure. The IIM method presents the maximum value of absolute error, which is about 0.23 in 4 different finite elements. The DK with linear spline covariance function presents a maximum value of absolute error equal to 0.20 in 12 different finite elements, while the DK with cubic spline covariance function presents a maximum value of absolute error equal to 0.13 in 16 different elements. The minimum values of the error are symmetric in value to the maximum values but located at different elements. This is consequence of the symmetry observed in the adopted distribution of the state variable (see Fig. 1 (a)).

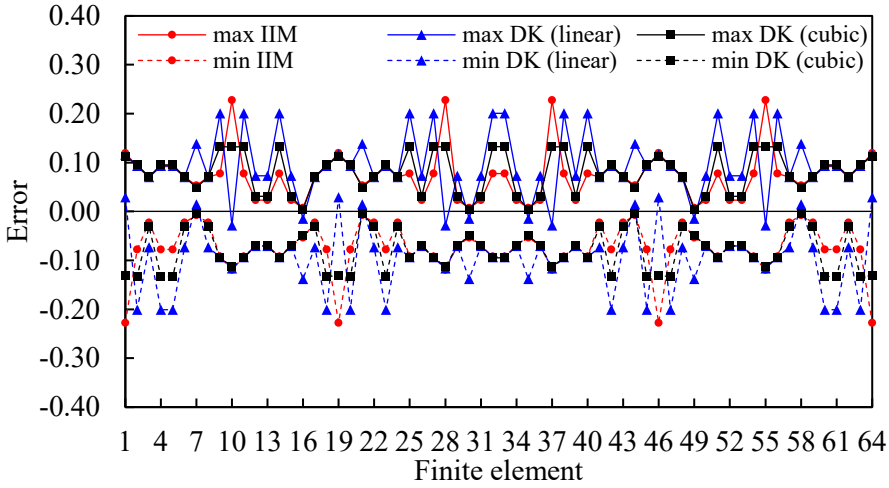

Fig. 4 – Maximum and minimum error value in each element after the refinement procedure.

Fig. 5 (a), (b) and (c) present the error distribution obtained after refinement procedure with the IIM method, DK with linear spline covariance function and DK with cubic spline covariance function method, respectively. The maximum and minimum error values generated by the IIM method are located towards the most outer nodes of the refined region. The DK with linear spline covariance function provides a cross pattern over each face of the refined volume. The maximum error values are adjacent to the minimum error values. The DK with cubic spline covariance function gives the global lower error values, which is in accordance with the results presented in Fig. 4.

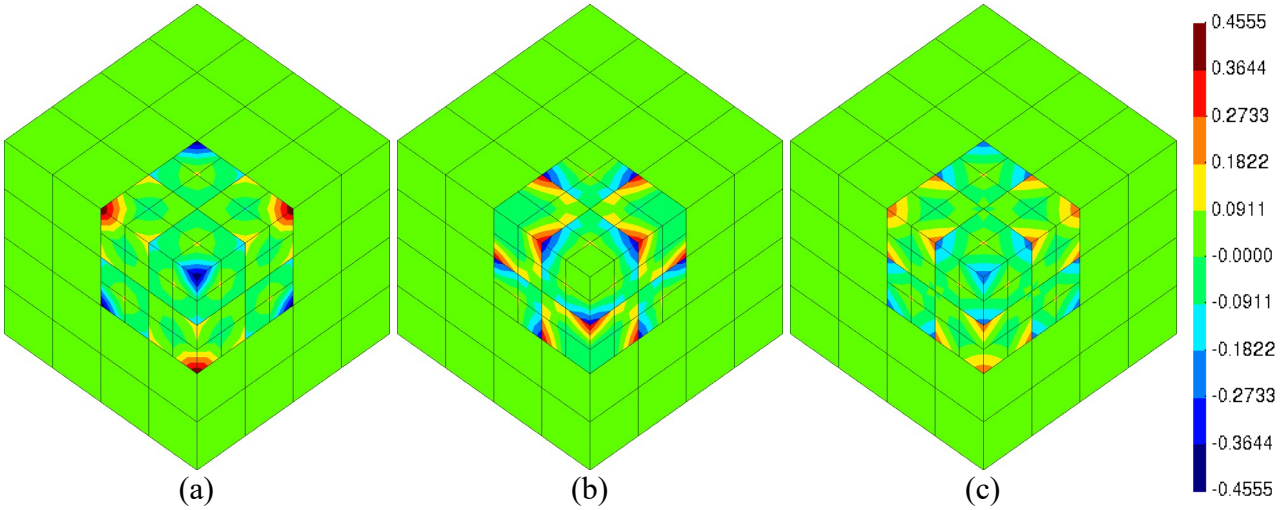

Fig. 5 – Error distribution obtained after refinement procedure: (a) IIM method, (b) DK with linear spline covariance function and (c) DK with cubic spline covariance function.

Error propagation. The error propagation was evaluated by performing the coarsening and decoarsening several times consecutively with the intent of alternating between the initial mesh and the coarsened mesh. An identical procedure was carried out for the refinement/derefinement procedure.

Fig. 6 (a) presents the maximum absolute error observed in each stage of 10 cycles of refinement/derefinement procedure applied to the initial mesh (see Fig. 1). The accuracy of the IIM method was independent of the analysed cycle, presenting a maximum absolute error after each refinement procedure of 0.23 and negligible error after derefinement procedure. On the other hand, both the DK with linear and cubic spline covariance functions displayed error propagation. The maximum absolute error increased significantly during the four first cycles and then stabilised for DK with linear spline covariance function, while with cubic spline covariance function, the absolute error increases approximately linearly with the number of stages. However, the DK with cubic spline covariance function presents the lowest maximum error value.

Fig. 6 (b) presents the maximum absolute error observed in each stage of 10 cycles of coarsening/decoarsening applied to the initial mesh (see Fig. 1). The IIM method is insensitive to the coarsening/decoarsening cycles, presenting an absolute error value of 0.18 after coarsening and 0.08 after decoarsening. The DK with linear and cubic covariance function displayed similar behaviour to the one observed in Fig. 6 (a). However, globally the increase of the error is significantly higher.

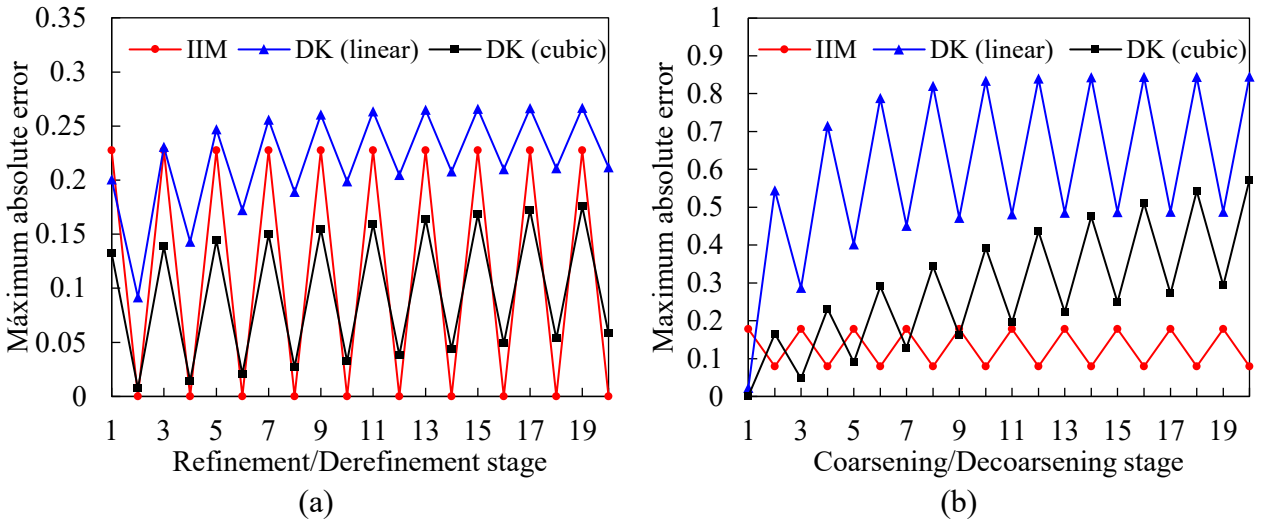

Fig. 6 – Maximum error observed for each stage: (a) 10 cycles of refinement/derefinement; (b) 10 cycles of coarsening/decoarsening.

Conclusions

The accuracy of each remapping method was evaluated both in the refinement and coarsening stages, obtaining distinct values due to the resolution of the final mesh. The accuracy of the remapping methods was lower in the refinement in comparison with the coarsening. In addition, the effect of the covariance function on the DK method has a significant impact on the accuracy. In all results, performance of the DK with cubic spline covariance function is better than the DK with linear spline covariance function. Overall, the error in the approximation of the state variable is lower using the DK method compared with the IIM method. However, the IIM method, unlike the DK method, does not suffer from error propagation.

Acknowledgements

The authors gratefully acknowledge the financial support of the projects POCI-01-0145-FEDER-031657 (PTDC/EME-EME/31657/2017) and UIDB/00285/2020 financed by the Operational Program for Competitiveness and Internationalization, in its FEDER/FNR component, and the Portuguese Foundation of Science and Technology (FCT), in its State Budget component (OE). The first author is also grateful to the FCT for the PhD grant with reference 2020.05267.BD.

References

[1] Herzog, D., Seyda, V., Wycisk, E., Emmelmann, C., Additive manufacturing of metals. *Acta Mater.* 2016, 117, 371–392.

[2] Gibson, I., Rosen, D., Stucker, B., Additive Manufacturing Technologies: 3D Printing, Rapid Prototyping, and Direct Digital Manufacturing, Second Edition. 2015.

[3] Neiva, E., Badia, S., Martín, A. F., Chiumenti, M., A scalable parallel finite element framework for growing geometries. Application to metal additive manufacturing. *Int. J. Numer. Methods Eng.* 2019, 119, 1098–1125.

[4] Eiser, S., Kaltenbacher, M., Nelhiebel, M., 2013 14th International Conference on Thermal, Mechanical and Multi-Physics Simulation and Experiments in Microelectronics and Microsystems, EuroSimE 2013. 2013.

[5] Bucher, A., Meyer, A., Görke, U. J., Kreißig, R., A comparison of mapping algorithms for hierarchical adaptive FEM in finite elasto-plasticity. *Comput. Mech.* 2007, 39, 521–536.

[6] Jiao, X., Heath, M. T., Common-refinement-based data transfer between non-matching meshes in multiphysics simulations. *Int. J. Numer. Methods Eng.* 2004, 61, 2402–2427.

[7] Murti, V., Wang, Y., Valliappan, S., Numerical inverse isoparametric mapping in 3D FEM. *Comput. Struct.* 1988, 29, 611–622.

[8] Yuan, K. Y., Huang, Y. S., Yang, H. T., Pian, T. H. H., The inverse mapping and distortion measures for 8-node hexahedral isoparametric elements. *Comput. Mech.* 1994, 14, 189–199.

[9] Poirier, C., Tinawi, R., Finite element stress tensor fields interpolation and manipulation using 3D dual kriging. *Comput. Struct.* 1991, 40, 211–222.